ELSEVIER

Physica D 121 (1998) 109–126

PHYSICA D

Localization and equipartition of energy in the β-FPU chain: Chaotic breathers

Thierry Cretegny [a,b], Thierry Dauxois [a,b,*], Stefano Ruffo [a,1], Alessandro Torcini [a,2]

[a] *Dipartimento di Energetica "S. Stecco", Università di Firenze, via S. Marta, 3 , I-50139 Firenze, Italy*

[b] *Laboratoire de Physique, URA-CNRS 1325, ENS Lyon, 46 Allée d'Italie, 69364 Lyon Cédex 07, France*

Received 23 September 1997; received in revised form 5 March 1998; accepted 30 March 1998
Communicated by J.D. Meiss

Abstract

The evolution towards equipartition in the β-FPU chain is studied considering as initial condition the highest frequency mode. Above an analytically derived energy threshold, this zone-boundary mode is shown to be modulationally unstable and to give rise to a striking localization process. The spontaneously created excitations have strong similarity with moving exact breathers solutions. But they have a finite lifetime and their dynamics is chaotic. These chaotic breathers are able to collect very efficiently the energy in the chain. Therefore their size grows in time and they can transport a very large quantity of energy. These features can be explained analyzing the dynamics of perturbed exact breathers of the FPU chain. In particular, a close connection between the Lyapunov spectrum of the chaotic breathers and the Floquet spectrum of the exact ones has been found. The emergence of chaotic breathers is convincingly explained by the absorption of high frequency phonons whereas a breather's metastability is for the first time identified. The lifetime of the chaotic breather is related to the time necessary for the system to reach equipartition. The equipartition time turns out to be dependent on the system energy density ε only. Moreover, such time diverges as ε^{-2} in the limit $\varepsilon \to 0$ and vanishes as $\varepsilon^{-1/4}$ for $\varepsilon \to \infty$. © 1998 Elsevier Science B.V.

Keywords: Hamiltonian systems; Fermi–Pasta–Ulam model; Breathers; Energy localization; Energy equipartition; Chaotic dynamics

1. Introduction

In 1955, in one of the first but well-known numerical simulations, Fermi, Pasta and Ulam (FPU) [1] have observed the *absence* of thermalization in a nonlinear lattice in which the energy was initially fed into the lowest frequency mode. Even if a lot of progress have been made [2] in the last 30 years on the study of the evolution towards energy equipartition among linear normal modes, several points are far from being clarified. For historical reasons, the evolution towards equipartition has been usually analyzed considering an initial state where all the energy of

* Corresponding author. Address: Laboratoire de Physique, URA-CNRS 1325, ENS Lyon, 46 Allée d'Italie, 69364 Lyon Cédex 07, France. Tel.: +33 4 72 72 81 38; fax: +33 4 72 72 80 80; e-mail: tdauxois@physique.ens-lyon.fr.

[1] INFN and INFM, Firenze (Italy).

[2] INFM, Firenze (Italy).

PII S0167-2789(98)00107-9

the system was concentrated in a small packet of modes centered around some low frequency [2,3]. Only a few studies have been devoted to the evolution from an initial condition where all the energy was fed in the highest frequency mode [4,5]. From these analyses it turned out that this different initial condition leads to a completely new dynamical behavior in the transient time preceding the final equipartition. In particular, the main finding was the appearance of a sharp localized mode during the transient [4]. Moreover, the highest frequency mode turns out to be a linearly unstable periodic solution; thus, starting the orbit from this initial point in phase-space put the system on a hyperbolic point embedded into a chaotic layer. On the other hand, when low frequency modes are initially excited, instability arises because of the presence of thin chaotic layers near elliptic points [6]. Therefore, we expect that the timescales for the relaxation to the equipartition state and the physical picture of the evolution towards the final state should be strongly affected.

In this paper, we present a detailed numerical and theoretical study of the dynamics of a β-FPU model in the transient preceding equipartition, when only the highest frequency mode is initially excited. Employing the quite recent concept of breather excitations [7], we are able to give a more detailed explanation of some of the behaviors observed in [4]. In particular, we show that the existence of such localized modes during the transient is strongly connected to exact breather modes for the β-FPU model (for a review on breathers, see [8]). An important peculiarity of these excitations is that (contrary to exact breathers) they have a chaotic evolution in time, therefore we have termed them "chaotic breathers" (CBs). The fact that localized oscillating excitations (that can be identified as CBs) show up spontaneously [9,10] and persist in numerical simulations has suggested that they play an important role in the dynamics of Hamiltonian anharmonic systems. However, an important point that should be clarified is why these objects emerge so easily in Hamiltonian systems. Since Hamiltonian dynamics is reversible, large packets should break up into smaller ones at the same rate that small ones merge into larger one; while in the formation of a CB the latter process seems to be favored. It is one of the purposes of this paper to give some clarification about these points and in particular to emphasize the importance of these localized excitations for the transition towards energy equipartition.

Another important aspect that we discuss is the existence of scaling laws for the indicators characterizing the approach to the equipartition state. We notice that quite general scaling laws indeed exist in the thermodynamic limit. Moreover, the relevant quantity for the equipartition time turns out to be the energy density.

We have organized the paper in the following way. The results of numerical simulations concerning the appearance of CBs are presented in Section 2. The consequences of the existence of CBs for the transition to equipartition are presented in Section 3 together with the observed scaling laws. The relation between CBs and exact breathers is discussed in detail in Section 4. Finally, Section 5 will deal with the mechanisms of creation and destruction of breathers. Some final remarks and conclusions are reported in Section 6.

2. Modulational instability and energy localization

Denoting by $u_n(t)$ the position of the nth atom ($n \in [1, N]$), the equations of motion of the β-FPU chain read

$$\ddot{u}_n = u_{n+1} + u_{n-1} - 2u_n + \beta\,[(u_{n+1} - u_n)^3 - (u_n - u_{n-1})^3], \tag{1}$$

where $\beta = 0.1$. The parameter β can be absorbed with an appropriate rescaling of u_n, but we keep it not only for historical reasons, but also in order to make easier comparisons with results reported in previous papers. We have chosen periodic boundary conditions which allow the propagation of waves in the lattice. As recently shown in [11], the study of the evolution of traveling waves with wavelength of the order of the system size (i.e. $\simeq N$) can give very useful information. In particular, the average lifetime of such waves is strictly related to the time necessary to reach equipartition. Here again, the propagation of waves and localized structures will play a fundamental role in the evolution of the system.

As usual, in numerical simulations one does not study the real Hamiltonian system, but a discrete time version that approximates the time continuous dynamics. It is therefore essential for long time simulations to use an appropriate symplectic integration scheme in order to preserve as far as possible the Hamiltonian structure of the problem. We adopt the sixth-order Yoshida's algorithm [12] with a time step $\mathrm{d}t = 0.01$; this choice allows us to obtain an energy conservation with an accuracy $\Delta E \simeq 10^{-11}$ (that corresponds to a relative accuracy $\Delta E/E$ ranging from 10^{-10} to 10^{-12}).

We follow the approach proposed by Fermi–Pasta–Ulam in [1] where they look at the stability of one normal mode of the harmonic part, but contrary to them we have performed simulations adopting as initial condition the highest frequency mode. The highest frequency mode (the so called π-mode) corresponds to the following zig-zag pattern for u_n

$$u_n = (-1)^n\, a \quad \text{and} \quad \dot{u}_n = 0, \tag{2}$$

where a is its amplitude. Since most of the normal modes of the harmonic part of the Hamiltonian are no longer solutions of the full Hamiltonian, energy initially fed into one single mode will be shared on later times among other modes. However, this is not true for three particular modes that are exact solutions of the FPU lattice [13]. As the π-mode is one of these solutions, in order to destabilize such initial state a small amount of noise (of order 10^{-14}) has been added on the velocities.

As already shown in [5,14] the π-mode turns out to be modulational unstable above a critical energy E_c, that can be analytically derived [14]

$$E_\mathrm{c} = \frac{2N}{9\beta} \sin^2\left(\frac{\pi}{N}\right) \frac{7\cos^2(\pi/N) - 1}{(3\cos^2(\pi/N) - 1)^2}. \tag{3}$$

As for this mode, $E = N(2a^2 + 4\beta a^4)$, we easily see that if

$$a > a_\mathrm{c} = \sin(\pi/N)/\sqrt{\beta(9\cos^2(\pi/N) - 3)}, \tag{4}$$

the π-mode will be destroyed by modulational instability.

In Fig. 1(a) a generic evolution of the above initial state for $a > a_\mathrm{c}$ is reported. The grey scale refers to the energy residing on site n,

$$E_n = \tfrac{1}{2}\dot{u}_n^2 + \tfrac{1}{2}V(u_{n+1} - u_n) + \tfrac{1}{2}V(u_n - u_{n-1}), \tag{5}$$

where the substrate potential is $V(x) = \frac{1}{2}x^2 + \frac{\beta}{4}x^4$. Figs. 1(b), (c) and (d) refer to three successive snapshots of the local energy E_n along the chain. After a very short delay, a slight modulation of the energy in the system appears (see Fig. 1(b)) and the π-mode is destabilized. Later, as attested by Fig. 1(a), only a few localized energy packets emerge from this temporary state; they correspond to oscillating localized waves and are usually called breathers or intrinsic localized modes. At this stage, as inelastic collisions of breathers have a systematic tendency to favor the growth of big breathers at the expense of small ones [9,15], the number of localized objects decreases and only one very large amplitude breather-like excitation survives (see Fig. 1(c)): this is the excitation we have termed CB. The CB moves along the lattice with a perturbed ballistic motion: sometimes the CB is even stopped or reflected. During its motion the CB collects energy from the visited sites on the chain, and its amplitude increases. It is important to note that the CB will never be at rest and that it propagates in general with almost the same speed (in modulus). Finally, after a very long time and through a mechanism we will consider later, the CB decays and the system reaches the equipartition of energy, as illustrated in Fig. 1(d).

The main important aspect that arises from the above reported picture is that the dynamics of the model seems to favor the emergence of a well-localized state (CB) during the transient preceding equipartition [4].

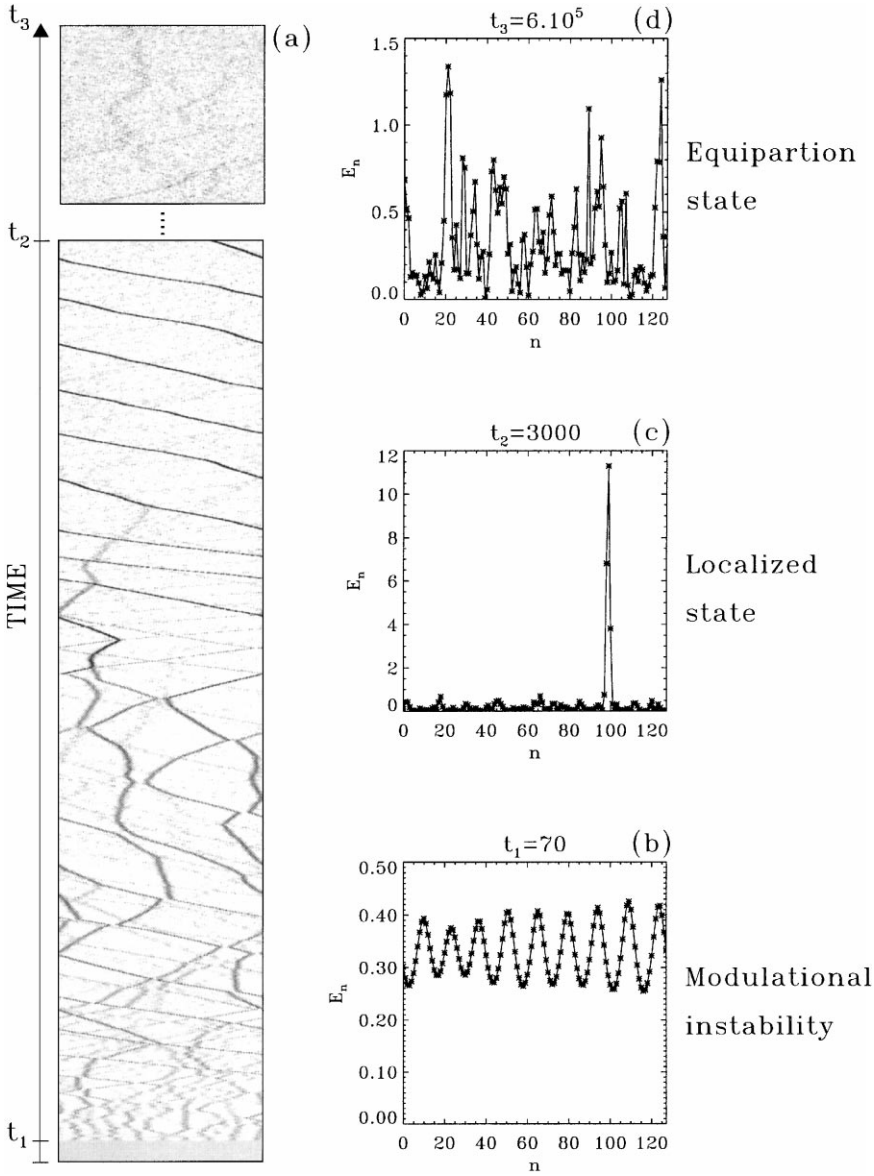

Fig. 1. Evolution of the local energy E_n along the chain. In (a), the horizontal axis indicates the position along the chain and the vertical axis corresponds to time (time is going upward). The grey scale goes from $E_n = 0$ (white) to the maximum E_n-value (black). The lower rectangle corresponds to $0 < t < 3000$ and the upper one to $5.994 \cdot 10^5 < t < 6 \cdot 10^5$; (b)–(d) show the instantaneous E_n along the $N = 128$ chain at three different times. Note the difference in vertical amplitude. The initial π-mode amplitude was $a = 0.4$ (while $a_c = 0.0317$).

In order to give a more quantitative characterization of the energy localization, we introduce the following quantity:

$$C_0(t) = N \frac{\sum_{i=1}^{N} E_i^2}{\left(\sum_{i=1}^{N} E_i\right)^2}. \tag{6}$$

As it can be easily seen C_0 is of order one if $E_i = E/N$ at each site of the chain and of order N if the energy is localized on only one site. In Fig. 2 C_0 is reported as a function of time for an initial condition (2) with $a > a_c$. Initially C_0 grows in time, indicating that the energy, evenly distributed on the lattice at $t = 0$, localizes over a few sites. This localized state survives for some time, at later times C_0 begins to decrease and finally it reaches an asymptotic value $\bar{C}_0$ that is associated with a total disappearance of the CB. At this stage a state with a flat distribution of energy in Fourier space is attained, i.e. a state where equipartition of energy is fulfilled. Already at this point, it is important to remark that for N greater than 512, all the curves $C_0(t)$ are almost coincident at any time. We discuss this point in Section 5.

The asymptotic value $\bar{C}_0$ can be easily obtained. In the limit $t \to \infty$, the energy per site has a mean value $\varepsilon = E/N$, but with some site dependent fluctuations, therefore $\bar{C}_0 = \langle E_i^2 \rangle / \langle E_i \rangle^2$. $\bar{C}_0$ can be theoretically estimated within a canonical ensemble picture, that allows us to derive an expression for $\langle E_i^2 \rangle$ (more details are reported in Appendix A). The actual $\bar{C}_0$-value depends on energy density ε and lies of course between the two limiting values: corresponding to the pure harmonic case $\bar{C}_0 = 7/4$ and the pure quartic case $\bar{C}_0 = 19/9$ (notice that both these values are independent of ε). As derived in Appendix A, for $\varepsilon = 1.44$, we obtain $\bar{C}_0 \simeq 1.795$, in perfect agreement with the numerical results as shown in Fig. 2.

3. Transition to the energy-equipartition state

In Section 2 we have shown that the energy-equipartition state is preceded by a transient characterized by the emergence of a localized state. The main properties of this state and its relationship with exact breathers are studied

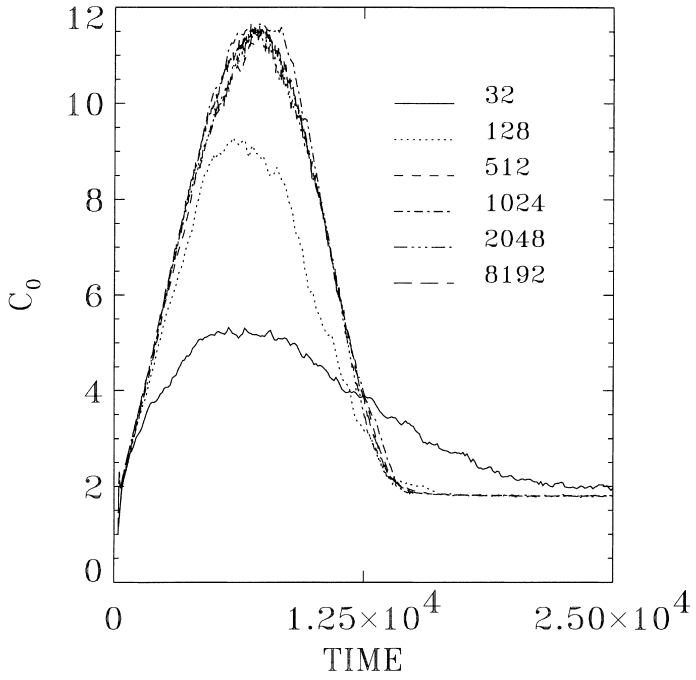

Fig. 2. Evolution of $C_0(t)$ for chains of various lengths: $N = 32$, 128, 512, 1024, 2048 and 8192. Each curve corresponds to the average over 20 simulations with the same energy density $\varepsilon = E/N = 1.44$ but with different random initial noise added to the velocities. For all the reported simulations $E > E_c$ (see footnote 3).

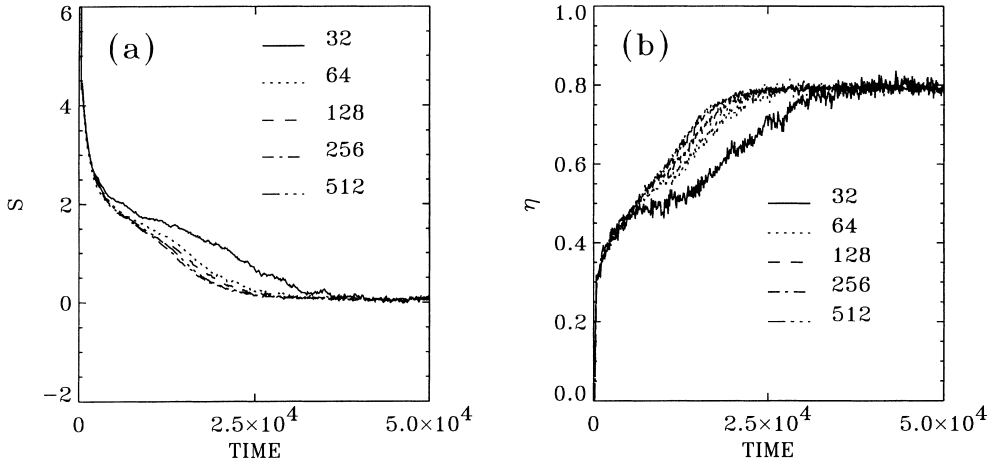

Fig. 3. (a) (resp. (b)) Presents the evolution of the slope $S(t)$ (resp. $\eta(t)$) versus time for chains of various lengths; N =32, 64, 128, 256 and 512. Each curve corresponds to the average over 20 different initial conditions with the same energy density $\varepsilon = 1.44$.

in the next section. Here we are mainly concerned with the identification of some general aspects of the transient. In particular, scaling laws for two indicators measuring the relaxation to thermodynamical equilibrium are derived.

As a first indicator we consider a parameter in the Fourier space $S(t)$ that gives a quantitative estimation of the energy transfer among the different normal modes [16]. The energy associated with the Fourier mode $q = 2\pi k/N$, with $k \in \{1 \dots N/2\}$, is in the harmonic approximation $\phi_q = \frac{1}{2}(|V_q|^2 + \omega(q)^2|X_q|^2)$, where $\omega(q) = 2\sin(q/2)$ represents the linear dispersion relation and V_q and X_q are the Fourier transforms of the velocities and the positions, respectively. Initially, all the energy is put in the π-mode, but as soon as the modulational instability develops also the nearest modes $q = \pi - \delta q$ acquire a non-zero amplitude ϕ_q, these numerical results confirm a previous analytical derivation of the most unstable modes [14]. After this initial stage, energy transfer from the highest modes to the lowest ones continues and the shape of the spectrum as a function of the wave vector is well described by an exponential

$$\phi_q \sim \exp[-S(t)(\pi - q)], \tag{7}$$

where, at any time t, $S(t)$ is the slope of the linear fit in the lin-log scale.

When the equipartition of energy is reached, the spectrum is no longer exponential (in other words the slope S vanishes). Therefore, the slope S is an excellent tool to follow the transition towards equipartition. The numerical results that we have obtained yield the interesting conclusion that the equipartition time is a function of the energy density ε only, as attested by Fig. 3(a), where all evolutions of $S(t)$ for various lengths are almost indistinguishable except for the smallest chain $N = 32$ where finite size effects do appear. [3]

Let us remark that in the original FPU problem, with excitations of long-wavelength modes, the distribution was well approximated by $\phi_q \sim \exp[-S(t)\, q]$. In that context, introducing the analytic continuation of the continuum field $u(x, t)$ to the complex plane [16], the slope was directly related to the imaginary part of the nearest singularity to the real axis. Work along this line would probably lead to a similar conclusion in our case.

The transition to equipartition can be investigated even more precisely considering the following indicator [17]:

$$\eta(t) = \frac{2}{N} \exp - \sum_q p_q(t) \ln p_q(t), \tag{8}$$

[3] $E_c(N)$ vanishes as N^{-1}, but $E_c(32) \simeq 1.04$ is not negligible for $\varepsilon = 1.44$.

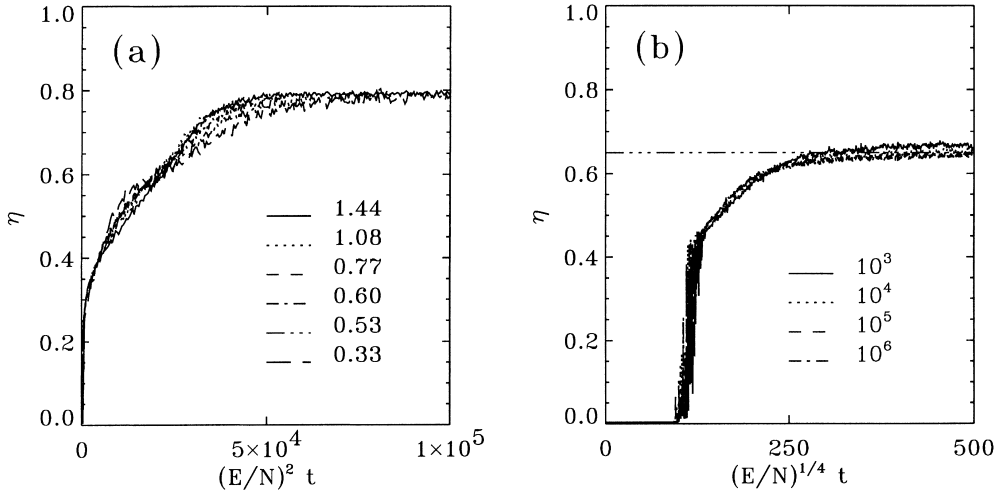

Fig. 4. In (a) (resp. (b)) the evolution of $\eta(t)$ versus the rescaled time $t(E/N)^2$ (resp. $t(E/N)^{1/4}$) is reported for different energy densities. Each curve in (a) (resp. (b)) corresponds to the average over 20 (resp. 50) different initial conditions for a chain with $N = 512$ sites. The dot–dashed line reported in (b) indicates the asymptotic value $\bar{\eta} \simeq 0.655$, which is theoretically estimated in Appendix B.

where $p_q(t)$ is the probability to have an energy ϕ_q associated to the mode q at time t; i.e.

$$p_q(t) = \phi_q \Big/ \sum_q \phi_q. \tag{9}$$

Indeed, $\eta(0) = 0$ whereas $\max(\eta) = 1$ is reached[4] in the energy equipartition state where all $p_q = 2/N$ (for a detailed derivation of the equipartition value $\bar{\eta}$ see Appendix B). Thus energy sharing among normal modes will be detected by an increase of $\eta(t)$, which can be considered as the percentage of modes with significant energy. It is exactly what we obtain in Fig. 3(b) for various chain lengths. The main conclusion that we can draw from this result is that again the equipartition time is a function of energy density ε only, and therefore it is finite in the thermodynamic limit, although it may diverge in the limit of vanishing energy density (see the following).

Simulations for various energy densities $0.33 \leq \varepsilon \leq 10^6$ allow us to study the variation of the equipartition time as a function of the the energy density. In the low energy limit ($0.33 \leq \varepsilon \leq 1.44$), a good data collapse is obtained if the time is rescaled by a typical time scale $\tau \sim \varepsilon^{-2}$ (see Fig. 4(a)). At high energy ($\varepsilon > 1000$) the typical timescale is $\tau \sim \varepsilon^{-1/4}$, as it is clearly shown in Fig. 4(b). Let us also stress that ε was also found to be the relevant dependence of the largest Lyapunov exponent in the equipartition state [14,18]. Moreover, the maximal Lyapunov exponent shows two scaling laws at high and low energy density that coincide with those here reported for the equipartition time (namely, for its inverse) [14,19]. However, while for the Lyapunov the transition from one regime to the other is observed at $\varepsilon \simeq \beta^{-1}$ [14,19], for the equipartition time the transition occurs at higher energy: $\varepsilon \simeq 100$ for $\beta = 0.1$. Power law divergences of the relaxation time have been recently reported for several models of nonlinear oscillators and for different classes of initial conditions [20–22], although the large N limit has not been studied as carefully as in the present paper.

[4] The asymptotic value $\bar{\eta}$, for low (resp. high) energy densities, is rather $\simeq 0.795$ (resp. $\simeq 0.655$) than 1 because of the fluctuations around the value $p_q = 2/N$. $\bar{\eta}$ shows a continuous transition from 0.795 to 0.655 for increasing ε. These discrepancies were already noticed in [38]. In Appendix B a more detailed analysis of this point is reported.

4. Relationship between exact and chaotic breathers

In the present section, we would like to pay attention to the localized objects observed during the transient state, and study their relationship with the already known localized solutions of nonlinear lattices, that we call *exact* breathers. We have seen that the energy contained in a CB (and thus its frequency) can be very high. For example, in chains of $N = 512$ sites, we found breathers with frequency $\omega \approx 3.5$ (when the maximal frequency associated to the phonon band is 2). We would like to emphasize here that the usually adopted Nonlinear Schrödinger approximation [4,23] is not appropriate to describe these objects.

The unstable π-mode gives rise spontaneously to a localized breather-like excitation, qualitatively very similar to the exact breathers obtained for the FPU chain [24]. The most evident difference is that the former move in an erratic way in the lattice and have a finite lifetime, while the latter are exactly periodic and mainly static. Therefore it is natural to try to determine to what extent it is possible to compare them.

Another important difference between the self-created excitation and the exact breathers concerns their dynamical stability, which has been investigated with the aid of a Lyapunov analysis. On one hand exact breathers are linearly stable and remain perfectly unchanged during very long simulations. On the other hand, we show here that CBs are strongly chaotic.

In order to compute the Lyapunov exponents of the system, we have used the standard algorithm of Benettin et al. [25]. However, we are here interested in the Lyapunov exponents at *short times* instead of the asymptotic ones. We evaluate the cumulative average corresponding to such exponents as a function of time. In Fig. 5, the evolution of the localization parameter $C_0(t)$ is reported (panel (a)) together with the corresponding cumulative average for the first four Lyapunov exponents (panel (b)) for a typical evolution starting from an unstable π-mode.

It is clear from Fig. 5(b) that the localized object, which has spontaneously appeared, is chaotic because its presence (indicated by the peak in $C_0(t)$) is associated with a positive maximal Lyapunov exponent. Moreover, another typical feature of the CB is that the running average for the maximal Lyapunov exponent has an higher

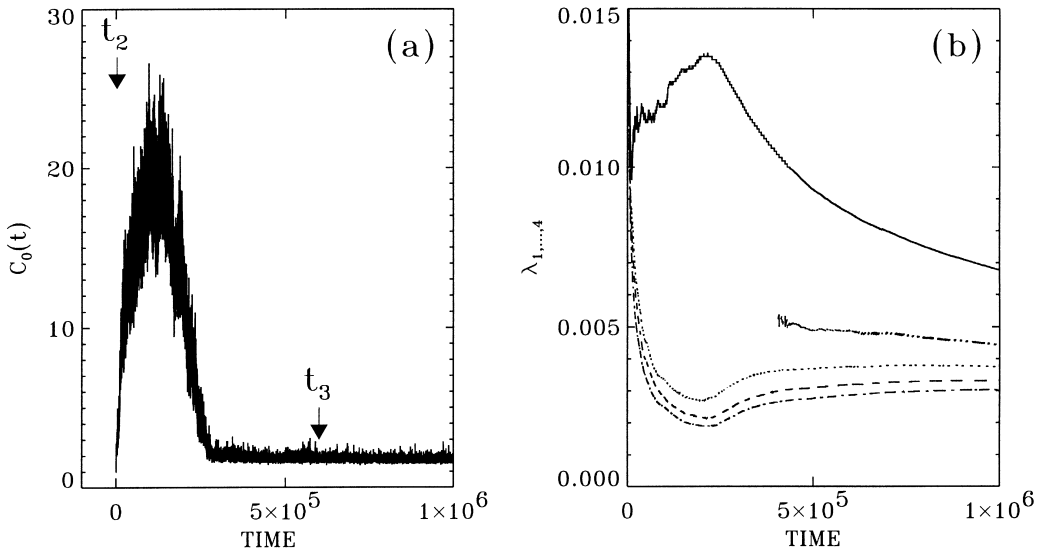

Fig. 5. (a) Presents the evolution of $C_0(t)$ and (b) presents the cumulative average of the first four Lyapunov exponents when the initial condition is a π-mode with $a = 0.4$ in an $N = 128$ chain. The solid line corresponds to the first Lyapunov exponent (the dash–triple dotted line corresponds to the value of the largest Lyapunov exponent after the transient), the dotted one to the second, the dashed one to the third and the dash–dotted line to the fourth. t_2 and t_3 in (a) are defined in Fig. 1.

value during the transient than in the equipartition state. The evolution of this running average is quite similar to that of $C_0(t)$: there is an initial growth followed by a decrease at later times. Naively, one would usually expect that an higher degree of chaoticity should be related to a higher degree of energy equipartition: the present simulations clearly shows the opposite.

One should stress that the running average for the Lyapunov exponents relaxes very slowly to the asymptotic value, because its value is affected by the estimation at earlier times. A more efficient method to obtain the asymptotic Lyapunov exponents is therefore to restart the running averages *after* the transition to equipartition state (i.e. after the decrease of C_0). The dash-triple dotted line of Fig. 5(b) shows that the convergence is much faster if this is done.

Another interesting result is the fact that a gap is present in the distribution of the Lyapunov exponents during the transient: the first Lyapunov is clearly above the others whereas, when the system reaches the energy equipartition state, the gap disappears (as shown in Fig. 5(b)) and the whole spectrum of Lyapunov exponents is approximately linear [26].

Furthermore, a measure of the localization of the Lyapunov vectors shows that during the transient the first Lyapunov vector is localized contrary to all others. This localization of the Lyapunov vector disappears after that the equipartition is reached, since the energy density is below the strong stochasticity threshold, see [14]. An interesting question is to see whether this peculiar structure of the tangent space (i.e. the gap in the spectrum and the localization of the first Lyapunov vector) can be related to the properties of exact breathers.

Let us briefly recall that exact discrete breathers are time-periodic and spatially exponentially localized solutions of the equations of motion (1). Their frequency is always higher than the frequency of the top of the phonon band. Calculating such a solution is equivalent to looking for a fixed point of the stroboscopic T map

$$(\{u_n, \dot{u}_n\})(0) \mapsto T(\{u_n, \dot{u}_n\}) = \{u_n, \dot{u}_n\}(t_b), \tag{10}$$

where t_b is the period of the solution. This can be done with the aid of a Newton process, using the tangent map ∂T. The latter relates linearly an initial perturbation $\{\epsilon_i, \dot{\epsilon}_i\}(0)$ to its image $\{\epsilon_i, \dot{\epsilon}_i\}(t_b)$ where the perturbations ϵ_i evolve according to the N linearized equations of motion

$$\ddot{\epsilon}_n = [1 + 3\beta(u_{n+1} - u_n)^2](\epsilon_{n+1} - \epsilon_n) - [1 + 3\beta(u_n - u_{n-1})^2](\epsilon_n - \epsilon_{n-1}). \tag{11}$$

Starting from a sufficiently good approximation, the Newton method converges to a periodic solution, satisfying Eq. (10) up to machine precision [24]. One can then investigate the linear stability of the breather solution with a standard Floquet analysis, i.e. computing the eigenvalues of the $2N \times 2N$ matrix ∂T (a periodic solution is linearly stable when all eigenvalues lie on the unit circle of the complex plane).

The main results concerning exact breathers in the FPU chain can be summarized as follows. They exist for every frequency above the phonon band; moreover the spatially antisymmetric solutions (centered between two particles, as the generic example plotted in Fig. 6(a) and sometimes called P-modes [27]) are linearly stable, while the symmetric (the ST-modes [28]) are unstable. The spectrum of the Floquet matrix, discussed in detail in [29], consists of a "continuum" of spatially extended eigenmodes (the linear phonons) and a discrete part with a spatially symmetric and exponentially localized mode. Due to the time reversibility of the solution, the real axis is a symmetry axis of the spectrum (if λ is an eigenvalue of ∂T, then λ^* is also an eigenvalue). Fig. 6(b) shows schematically half of the spectrum (the other half is its complex conjugate) with the continuum and the discrete localized mode. As the problem is solved for a *finite* chain, the continuum corresponds in reality to $(N - 1)$ modes with a higher density of modes close to the end of the band.

Such linear modes out of the phonon band and with opposite symmetry to the original solution have been observed and studied in the framework of Klein–Gordon chains. They are called *pinning* or *translation* modes [8,30,31]. Indeed, an excitation of the periodic solution in the direction of this mode produces an oscillation of the

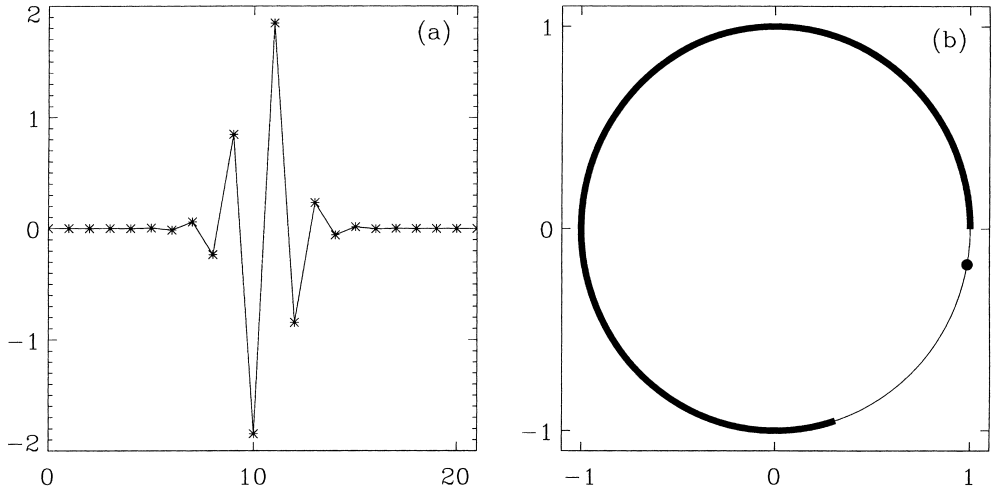

Fig. 6. (a) Presents the spatial shape of an exact linearly stable FPU breather, solution of Eq. (1) with a frequency $\omega = 2.5$; (b) shows the schematic repartition of its Floquet eigenvalues on the complex plane.

center of energy or can even lead to a propagation of the solution along the chain without radiative decay. We have checked that these features are also present in the β-FPU model.

The problem now is to link these exact solutions with the self-created excitations which have been observed in the simulations. The essential difference is that the former are linearly stable while the latter are strongly chaotic. However the comparison of the Lyapunov spectrum of the CB and the Floquet spectrum of the exact breather solution shows strong similarities: they both present a "continuum" of extended states and an isolated spatially localized mode. A quite natural hypothesis is that non-zero perturbations of the exact breather could lead to a strong destabilization of the translation mode. If this is true, one can understand why this instability is not destructive for the breather: a perturbation along this direction only leads to a coherent displacement of the breather and in addition, it explains why, in the simulations, the nonlinear excitation is very seldom static.

In order to verify that the most unstable direction corresponds to the translation mode of the exact solution, we have performed the following test. We study the evolution of an exact solution, once it has been perturbed with a spatially antisymmetric gaussian noise all over the lattice. The antisymmetry of the initial condition allows the breather to remain at rest centered between two sites and this simplifies the comparison. The Lyapunov analysis reveals that the perturbed state is now chaotic. The maximal Lyapunov eigenvector associated with the perturbed solution and the Floquet vector corresponding to the translational mode for the unperturbed case are shown in Fig. 7. The two vectors are both symmetric and in perfect agreement. This is a convincing evidence that the structure of the tangent space of a CB can be qualitatively interpreted in terms of the Floquet spectrum of "neighboring" exact periodic solutions.

We would like to stress that the fact that breather-like excitations move is not a sufficient condition for their chaoticity. Similarly to what has already been found numerically for Klein–Gordon chains [31], many exact mobile breather solutions can be exhibited by the FPU model (see [32–34] or [8] for a discussion on approximations of moving breathers). Such solutions satisfy the relation

$$\{u_n, \dot{u}_n\}(T) = \{u_{n-1}, \dot{u}_{n-1}\}(0), \tag{12}$$

where T, the inverse of the velocity, is a multiple of the period of internal vibration of the breather. One should also note that a small amplitude phonon tail dresses these solutions, such that one can consider that the breather is

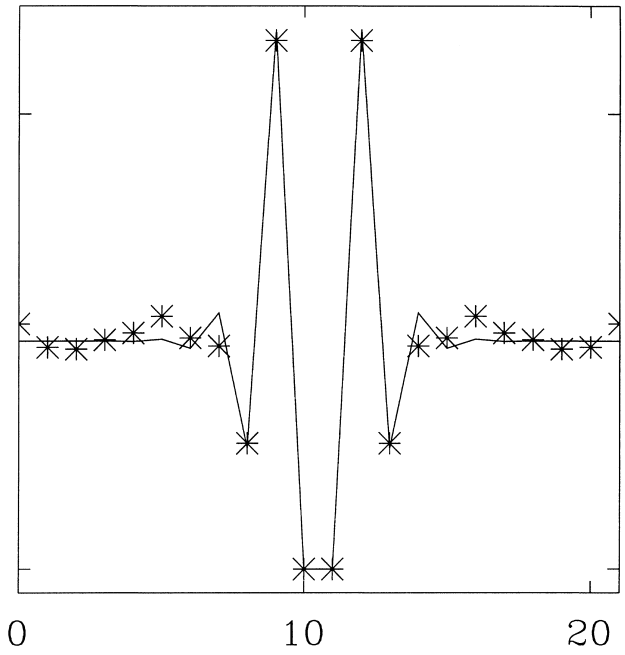

Fig. 7. Shape of the translation mode. The solid line corresponds to the eigenmode of the Floquet analysis whereas the stars correspond to the first Lyapunov eigenvector. We have reported only the part of the vectors relative to the positions when the internal phase of the breather is zero (i.e. when the kinetic energy is minimal).

in equilibrium with the emitted and the absorbed radiation (for more details see [31]). Many of these solutions are linearly stable and were checked to have zero maximal Lyapunov exponent; the chaotic regime is reached only if the whole system is sufficiently perturbed. The direction of the translation mode is easily excitable, but is not the direction responsible for chaoticity: thus mobile breathers are not necessarily chaotic and strong chaos occurs only when other modes are sufficiently excited.

5. Formation and destruction of breathers

At this stage, we have understood the connection of the CB with exact FPU breathers but we should explain how the destabilization of the π-mode can lead to only one localized solution. Indeed, as attested by Fig. 1(a), the modulational instability gives rise first to a few packets of energy but then, because of their interactions, energy is concentrated in only one.

5.1. The localization process

In order to study this effect in a controlled manner, we have put four exact breathers on the lattice: three moving ones with small amplitude and a frequency $\omega = 2.12$, that is just above the phonons' upper band edge ($\omega = 2$), and one at rest with a larger amplitude and a frequency $\omega = 2.75$. As shown in Fig. 8, due to collisions, the biggest breather successively absorbs the smaller ones and gives rise to a moving large amplitude breather-like excitation. Such a result is a generic example of the collision process in the FPU chain and it explains why a single localized CB emerges during the transient.

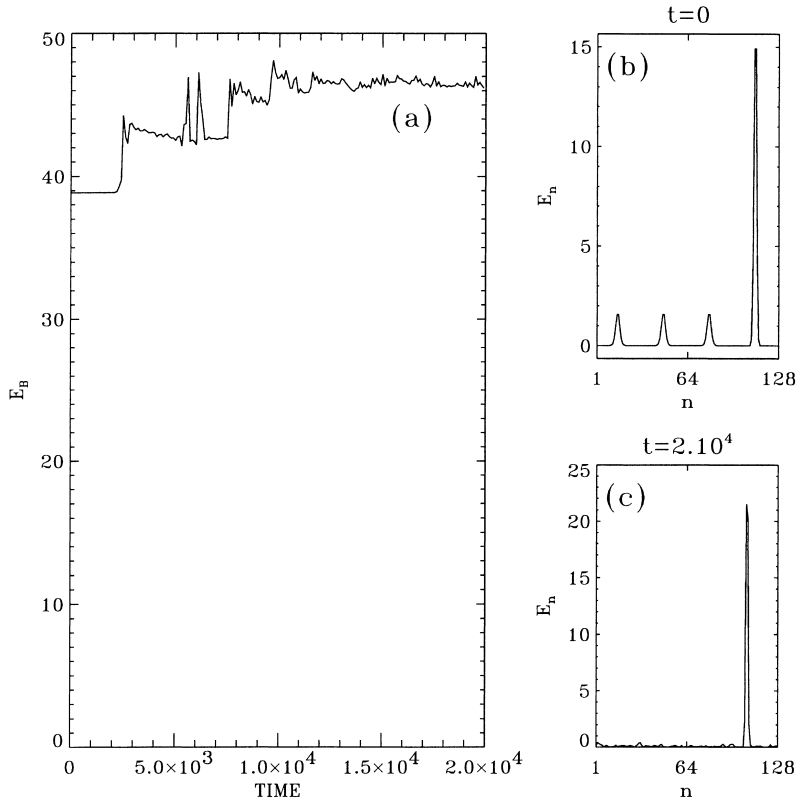

Fig. 8. Breathers' merging: (a) shows the energy evolution of an exact breather initially at rest ($\omega = 2.75$) after collisions with three small exact moving breathers ($\omega = 2.12$); (b) (resp. (c)) shows the energy repartition at $t = 0$ (resp. at $t = 2 \cdot 10^4$).

Let us emphasize that even if some localization processes have already been reported in homogeneous nonlinear lattices [9], the process presented here is particularly interesting because of the absence of the self-regulation process. Indeed, in the Klein–Gordon systems studied in [9,10], the process is regulated by a stronger pinning effect. Discreteness provides a path to localization but is also responsible for the pinning effect. This is stronger for larger excitations (big breathers are easier trapped), and this does not allow a collapse of all the breathers into a single very large excitation. For the FPU model, pinning effects are perhaps too small to be detected. Moreover, we have observed that the velocity of the CB slightly increases with its energy. As a consequence, we see in Fig. 1 the emergence of only one large amplitude breather-like excitation from the initial π-mode.

Is this effect present also in the thermodynamic limit ? As the lifetime τ and the velocity v of a CB are finite, one could predict that, for very long chains, the CB will probably not have enough time to collect all the energy present in the system. If, in small chains, the breather could easily move through the system many times, in very long chains this would not be the case. One can expect that above a critical chain length $L_c = v\tau$ more than one CB will be observed in the transient preceding equipartition. To check this, we have investigated the case with an initial amplitude $a = 0.8$ for the π-mode; in this situation the typical velocity of the final breather is $v \sim 0.2$ and its lifetime is $\tau \sim 10^4$. From these data the critical length L_c is $\sim 2 \cdot 10^3$. For chains $N > 10^3$ and $a = 0.8$, additional simulations have shown that this is indeed true: the energy is no longer localized in only one huge CB but in few of them.

A long chain could therefore be considered as a juxtaposition of almost non-interacting sub-chains of length L_c. And in each sub-chain, one single CB is created by the modulational instability. This interpretation is consistent with the observed saturation of the localization parameter C_0 when the size of the system increases (Fig. 2). Indeed, a chain can be considered as made up of two independent parts A and B, and one has $C_0(A+B) = (C_0(A)+C_0(B))/2 = C_0(A)$ (C_0 is an intensive-like quantity). As discussed in Section 3, the lifetime is a function of the energy density ε. Thus the critical length of course depends on ε.

One can define two different regimes associated to the growth of the excitation. In a first stage the main breather present in the chain absorbs the smaller ones by collisions. After this initial stage the growth slows down. This effect could be explained by an observation made by Bang and Peyrard for the Klein–Gordon equation [15]. They noticed that the energy transfer between localized modes depends on their relative energy difference: the transfer is less efficient when the energy difference (or frequency difference) increases. For our system we have observed that, after the first collisions, the lattice contains one big breather with a rather high frequency and a large population of high frequency phonons waves. The presence of the latter is due to the destabilization of the original π-mode via modulational instability [14]. Correspondingly, the energy transfer-rate between the phonons and the CB is still positive but reduced with respect to the initial one. We want to stress that this second regime was detected because of the very small initial perturbations of the π-mode, since for bigger perturbation this regime can easily be missed [4]. In addition, in this paper we have concentrated our attention on the energy region just above the critical energy defined by Eq. (3), where the FPU chain evolves towards equipartition on a very long time scale.

5.2. Breather's metastability

Once the localization process is finished, a very large amplitude breather is moving in the system and all the high frequency waves have been absorbed. The hungry excitation cannot grow any more and this regime corresponds to the plateau where C_0 has reached its maximum. At later times, the excitation disappears and now we want to explain how this phenomenon can take place. We have seen that the effect of collisions of the CB with high frequency modes leads to absorption of the latter. During such a scattering process, small quantities of energy radiate towards low frequency modes. Therefore, after the initial stage the only phonons left in the system are the low frequency ones. It is natural to suspect that the destruction of the CB is related to their interaction with the low frequency modes.

In order to understand this interaction, we have performed numerical experiments where one exact breather initially at rest collides with the following wave packets of low frequency phonons centered on the site n_0:

$$u_n(t) = A\cos(qn - \omega t)\mathrm{e}^{-(n-n_0)^2/2l_0^2}. \tag{13}$$

We have taken $q = 0.2$, $l_0 = 13$ and an amplitude $A \in [0.5; 3]$. Fig. 9 shows that the collision process is very efficient in destroying the CB excitation.

As shown in Fig. 9(a), the decrease of the energy of the breather E_B can be considered as linear at the earlier times with a good approximation. Moreover, a more detailed study of the phenomenon shows that the amplitude of the wave packet determines the destruction rate. In particular, the slope of the decrease of E_B is an exponential function of the amplitude. This result suggests that a very complicated nonlinear mechanism is at the origin of the interaction. To give a more quantitative explanation we should study the scattering on one phonon with the CB as done by Cretegny et al. [29] for exact breathers at rest in the Klein–Gordon model. However, here, the study will be much more complicated because small perturbations will easily put the FPU-breather in motion.

A possible explanation of the CBs metastability is the following: at the beginning of the simulation, when only the π-mode is excited, and even during the modulational instability process, the low frequency phonons are not present. During the growing process of the CB the low frequency phonon band is populated due to radiative processes. When all the high frequency phonons have been absorbed by the CB, the excitation can only loose energy due to

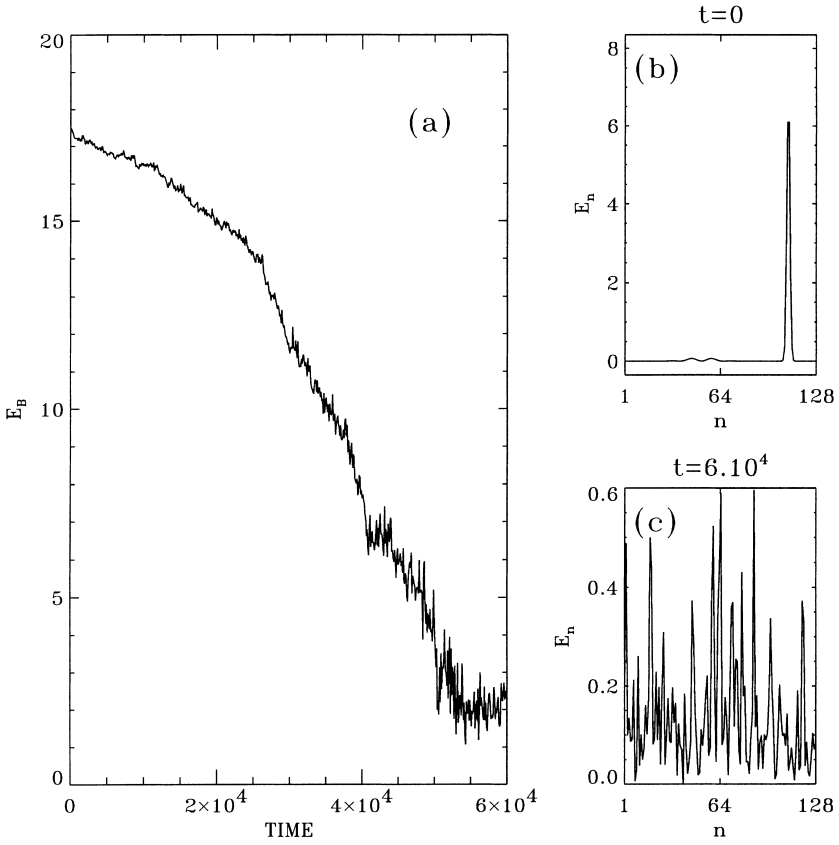

Fig. 9. Breathers' destruction: (a) shows the evolution of the energy of an initial exact static breather ($\omega = 2.4$) after collisions with a wave packet of phonons ($A = 1.5, l_0 = 13,\ q = 0.2$); (b) (resp. (c)) shows the initial (resp. final) repartition of energy.

the destructive interaction with the low frequency phonons. Therefore, we can say that the CB "die of starvation". The destruction of the CB is associated with a significant increase in the population of low frequency linear waves. This transition corresponds to the final decrease of the slope $S(t)$ plotted in Fig. 3 and to the final relaxation to the equipartition state.

6. Conclusion

We have seen that the evolution towards equipartition in the β-FPU chain, starting from the π-mode as initial condition, gives rise to a striking localization process. The spontaneously created excitations are moving breather-like excitations with a finite lifetime and a chaotic dynamics. The features of these transient localized modes can be explained by exploiting the correspondence with exact breathers.

It is important to recall that the FPU equation was at the origin of the rediscovery of the soliton [35] in the continuum limit, which justified the recurrence phenomenon observed by Fermi–Pasta–Ulam [1] (see also [36]). In the present paper, we have shown the fundamental role played by a second family of excitations, the breathers, in achieving the equipartition state on a discrete FPU lattice. The creation of a CB can be considered as an efficient mechanism to transfer energy from high frequency modes to low frequency phonons.

Let us also remark that the breathers are created from the high frequency zone corresponding to zero group velocity. This portion of the phonon band was also recently found to be crucial for the transition to equipartition [37]. Indeed, the transition to equipartition disappears if a renormalized FPU Hamiltonian with a dispersion relation without zero group velocity region is considered [37]. As in electromagnetism and string theory, the idea that this ingredient is absolutely necessary to observe the transition to equipartition of energy is another reason to justify a posteriori our study.

Moreover, we have found that the fundamental parameter for the dynamics of the system is always the energy density $\varepsilon = E/N$ (i.e. energy/volume). This is true not only for the value of the maximal Lyapunov exponent (as already noticed in [14,18]) but also for the transient time towards energy equipartition. One should of course emphasize that this is the only parameter which makes sense in the thermodynamic limit. Therefore, the transition to equipartition happens in a finite time in the thermodynamic limit, but this time diverges as an inverse power of the energy density in the zero energy density (zero temperature) limit.

As a final remark, this study emphasizes that the concept of a breather is not only important for the energy localization in lattices, but is also crucial to address one of the main classical problem of statistical mechanics: the transition to equipartition.

Acknowledgements

TC is supported by “le Conseil de la Région Rhône-Alpes” with a grant “Emergence”. TD gratefully acknowledges EC for financial support with grant ERBFMBICT961063. This work is also part of the European contract ERBCHRXCT940460 on “Stability and universality in classical mechanics”. SR acknowledges the hospitality of the *Centro Internacional de Ciencias* in Cuernavaca, Mexico and the financial support of the same Center and of CONACYT. AT thanks the University of Wuppertal (Germany) and the Ecole Normale Supérieure of Lyon (France) for the nice hospitality. We would like to thank S. Aubry, R. Livi and M. Peyrard for a careful reading of this manuscript. Part of CPU time has been nicely supplied by the Institute of Scientific Interchanges (ISI) of Torino.

Appendix A. Calculation of the equipartition value $\bar{C}_0$ of the localization parameter

Introducing the usual parameter $\beta = 1/k_B T$, we obtain directly from Eq. (6), the asymptotic expression corresponding to energy equipartition

$$\bar{C}_0 = N \frac{\sum_i E_i^2}{\left[\sum_i E_i\right]^2} = \frac{\langle E_i^2 \rangle}{\langle E_i \rangle^2} \,, \tag{A.1}$$

where the spatial averages are

$$\langle E_i \rangle = \left\langle \frac{p_i^2}{2} + \frac{V_i}{2} + \frac{V_{i+1}}{2} \right\rangle = \frac{1}{2\beta} + \langle V_i \rangle \,, \tag{A.2}$$

and

$$\langle E_i^2 \rangle = \left\langle \left(\frac{p_i^2}{2} + \frac{V_i}{2} + \frac{V_{i+1}}{2} \right)^2 \right\rangle = \frac{3}{4\beta^2} + \frac{1}{\beta} \langle V_i \rangle + \frac{\langle V_i^2 \rangle}{2} + \frac{\langle V_i \rangle^2}{2}. \tag{A.3}$$

For long chains, we can evaluate $\langle E_i \rangle$ and $\langle E_i^2 \rangle$ using the canonical ensemble. Introducing the configurational partition function

$$F(\beta) = \int_{-\infty}^{+\infty} \exp\left[-\beta V(x)\right] \mathrm{d}x, \tag{A.4}$$

we have

$$\langle V_i \rangle = -\frac{1}{F}\frac{\partial F}{\partial \beta} \quad \text{and} \quad \langle V_i^2 \rangle = \frac{1}{F}\frac{\partial^2 F}{\partial \beta^2}.$$

One obtains therefore:

$$\langle E_i \rangle = \frac{1}{2\beta} - \frac{1}{F}\frac{\partial F}{\partial \beta} \tag{A.5}$$

and

$$\langle E_i^2 \rangle = \frac{3}{4\beta^2} - \frac{1}{\beta F}\frac{\partial F}{\partial \beta} + \frac{1}{2F^2}\left(\frac{\partial F}{\partial \beta}\right)^2 + \frac{1}{2F}\frac{\partial^2 F}{\partial \beta^2}. \tag{A.6}$$

In the pure harmonic case this gives $\langle E_i \rangle = 1/\beta$ and $\langle E_i^2 \rangle = 7/4\beta^2$, whereas in the pure quartic case we obtain $\langle E_i \rangle = 3/4\beta$ and $\langle E_i^2 \rangle = 19/16\beta^2$.

In conclusion, $\bar{C}_0 = \frac{7}{4}$ in the pure harmonic case and $\bar{C}_0 = \frac{19}{9} \simeq 2.11$ in the pure quartic case. But one can even compute the result using the complete FPU-potential. $V(x) = x^2/2 + \delta x^4/4$.

Using $\mathcal{K}_{1/4}$ the modified Bessel function of the second kind, we have

$$F(\beta) = \sqrt{\frac{1}{2\delta}} \mathrm{e}^{\beta/8\delta} \mathcal{K}_{1/4}\left(\frac{\beta}{8\delta}\right). \tag{A.7}$$

We obtain finally for $\delta = 0.1$, the value

$$\bar{C}_0 \simeq 1.795, \tag{A.8}$$

in excellent agreement with the numerical value.

Appendix B. Estimation of the equipartition value $\bar{\eta}$ in the harmonic approximation

We would like to give a theoretical estimation of the indicator $\eta(t)$ (see Eq. (8)) in the limit $t \to \infty$, i.e. in the equipartition state (the asymptotic value is indicated as $\lim_{t\to\infty} \eta(t) = \bar{\eta}$).

Let us rewrite the spectral entropy as

$$S = -\sum_{q=1}^{N/2} p_q(t) \ln p_q(t), \tag{B.1}$$

where $p_q(t) = \phi_q / \sum_q \phi_q$. Introducing the energy per mode $e = (2/N)\sum_{q=1}^{N/2} \phi_q$, in the equipartition state, we can easily derive the following expression:

$$S = -\frac{\langle \phi \ln \phi \rangle}{e} + \ln e + \ln\left(\frac{N}{2}\right). \tag{B.2}$$

The average appearing in (B.2) is $\langle \phi \ln \phi \rangle = (2/N) \sum_q \phi_q \ln \phi_q$, and due to the equipartition the index q has been neglected.

The corresponding expression for the quantity (8) is

$$\bar{\eta} = e, \quad \mathrm{e}^{-(1/e)\langle \phi \ln \phi \rangle}. \tag{B.3}$$

Assuming that the fluctuations can be neglected, we obtain

$$\langle \phi \ln \phi \rangle = \langle \phi \rangle \langle \ln \phi \rangle = \langle \phi \rangle \ln \langle \phi \rangle = e \ln e \tag{B.4}$$

and $\bar{\eta}$ would be exactly one. However, the numerical value of $\bar{\eta}$ estimated in the low energy limit is quite different from one (namely, it is $\simeq 0.795$). This indicates that the inclusion of the fluctuations is fundamental to give a realistic estimate of $\bar{\eta}$ (this was firstly noticed in [38]). In order to consider the fluctuations, let us write

$$\ln \phi = \lim_{n \to 0} \frac{\phi^n - 1}{n}. \tag{B.5}$$

This allows one to reexpress Eq. (B.4) as a function of average of powers of ϕ

$$\langle \phi \ln \phi \rangle = \lim_{n \to 0} \frac{\langle \phi^{n+1} \rangle - e}{n} \tag{B.6}$$

The estimation of $\bar{\eta}$ is now reduced to the estimation of terms of the type $\langle \phi^n \rangle$, which can be again evaluated within the canonical ensemble, after a mode inverse temperature β^* is introduced. In the harmonic approximation

$$\langle \phi^n \rangle = \left\langle \left(\frac{|V_q|^2 + \omega^2 |X_q|^2}{2} \right)^n \right\rangle = \sum_{k=0}^{n} \frac{n!}{k!(n-k)!} J_k J_{n-k} J_0^{-2}, \tag{B.7}$$

with

$$J_k = \int_{-\infty}^{+\infty} \mathrm{d}x \left(\frac{x^2}{2} \right)^k \mathrm{e}^{-\beta^* x^2/2} = \Gamma\left(k + \frac{1}{2} \right) \frac{\sqrt{2}}{(\beta^*)^{k+1/2}}, \tag{B.8}$$

where Γ is the Euler–Gamma function. In particular, $e = \langle \phi \rangle = (\beta^*)^{-1}$ and expression (B.7) reduces to

$$\langle \phi^n \rangle = e^n \Gamma(n+1) = e^n n!. \tag{B.9}$$

We are now able to give an expression for the spectral entropy.

$$\langle \phi \ln \phi \rangle = \lim_{n \to 0} \frac{e^{n+1} \Gamma(n+2) - e}{n} = e[\log(e) + \Gamma'(2)], \tag{B.10}$$

being $\Gamma'(2) = 1 - \gamma$, where $\gamma \simeq 0.5772$ is the Euler constant. Finally we obtain

$$\bar{\eta} = \mathrm{e}^{\gamma - 1} \simeq 0.655\,. \tag{B.11}$$

This results have been also obtained with a different approach in [38]. We notice that this value is in perfect agreement with the numerical one found in the high energy limit (see Fig. 4(b)), while it is an underestimation of the one found in the low energy limit (see Fig. 4(a)).

The origin of such a discrepancy is related to the structure of the Hamiltonian when expressed in terms of normal modes. Due to the quartic term in the potential, the mode interaction matrix is no longer diagonal [13]. However, in the high energy limit a sort of "random phase approximation" should be valid for the terms appearing in the

mode interaction matrix and the off-diagonal terms should average to zero. Therefore we are left, in the action-angle representation (I_q, θ_q), with diagonal terms of the form

$$H_{qq} = (\omega(q) I_q) + \frac{\beta^*}{2N} \omega(q)^2 I_q^2 \langle \cos^4 \theta_q \rangle. \tag{B.12}$$

In the limit $N \to \infty$ the nonlinear term in H_{qq} becomes negligible and the harmonic approximation is recovered.

In the low energy limit, the action–angle variables are strongly correlated and a "random phase approximation" is no longer valid. Therefore the off-diagonal terms cannot be neglected and give a contribution (although comparatively small) to $\bar{\eta}$.

References

[1] E. Fermi, J. Pasta, S. Ulam, Los Alamos Science Laboratory Report No. LA-1940 (1955), unpublished; in: E. Segré (Ed.), Collected Papers of Enrico Fermi, vol. 2, University of Chicago Press, Chicago, 1965, p. 978.
[2] J. Ford, Phys. Rep. 213 (1992) 271.
[3] A.J. Lichtenberg, M.A. Lieberman, Regular and Chaotic Dynamics, Springer, Berlin, 1992.
[4] V.M. Burlakov, S.A. Kiselev, V.I. Rupasov, Phys. Lett. A 147 (1990) 130; V.M. Burlakov, S. Kiselev, Sov. Phys. JETP 72 (1991) 854.
[5] K.W. Sandusky, J.B. Page, Phys. Rev. B 50 (1994) 866.
[6] F.M. Izrailev, B.V. Chirikov, Dokl. Akad. Nauk SSSR 166 (1966) 57 [Sov. Phys. Dokl. 11 (1966) 30].
[7] R.S. Mac Kay, S. Aubry, Nonlinearity 7 (1994) 1623.
[8] S. Flach, C.R. Willis, Phys. Rep. 295 (1998) 181.
[9] T. Dauxois, M. Peyrard, Phys. Rev. Lett. 70 (1993) 3935.
[10] I. Daumont, T. Dauxois, M. Peyrard, Nonlinearity 10 (1997) 617.
[11] P. Poggi, S. Ruffo, H. Kantz, Phys. Rev. E 52 (1995) 307.
[12] H. Yoshida, Phys. Lett. A 150 (1990) 262.
[13] P. Poggi, S. Ruffo, Physica D 103 (1997) 251.
[14] T. Dauxois, S. Ruffo, A. Torcini, Phys. Rev. 56 (1997) R6229.
[15] O. Bang, M. Peyrard, Phys. Rev. E 53 (1996) 4143.
[16] R. Livi et al., Phys. Rev. A 28 (1983) 3544.
[17] R. Livi et al., Phys. Rev. A 31A (1985) 1039.
[18] M. Pettini, M. Landolfi, Phys. Rev. A 41 (1990) 768.
[19] L. Casetti, R. Livi, M. Pettini, Phys. Rev. Lett. 74 (1995) 375.
[20] J. De Luca, A.J. Lichtenberg, S. Ruffo, Phys. Rev. E 51 (1995) 2877.
[21] L. Casetti, M. Cerruti-Sola, M. Pettini, E.G.D. Cohen, Phys. Rev. E 55 (1997) 6566.
[22] G. Parisi, Europhys. Lett. 40 (1997) 357.
[23] G.P. Berman, A.R. Kolovskii, Zh. Eksp. Teor. Fiz. 87 1938 (1984) [Sov. Phys. JETP 60 (1984) 1116].
[24] J.L. Marin, S. Aubry, Nonlinearity 9 (1996) 1501.
[25] G. Benettin et al., Meccanica 9 (1980) 21.
[26] R. Livi, A. Politi, S. Ruffo, J. Phys. A 19 (1986) 2033.
[27] J.B. Page, Phys. Rev. B 41 (1990) 7835.
[28] A.J. Sievers, S. Takeno, Phys. Rev. 61 (1988) 970.
[29] T. Cretegny, S. Aubry, S. Flach, Physica D 119 (1998) 73.
[30] D. Chen, S. Aubry, G. Tsironis, Phys. Rev. Lett. 77 (1996) 4776.
[31] S. Aubry, T. Cretegny, Physica D 119 (1998) 34.
[32] K. Hori, S. Takeno, J. Phys. Soc. Japan 61 (1992) 2181.
[33] S. Flach, C.R Willis, Phys. Rev. Lett. 72 (1994) 1777.
[34] P.A. Houle, Phys. Rev. E 56 (1997) 3657.
[35] N.J. Zabusky, M.D. Kruskal, Phys. Rev. Lett. 15 (1965) 240.
[36] C.Y. Lin, C.G. Goedde, S. Lichter, Phys. Lett. A 229 (1997) 367.
[37] D.L. Shepelyansky, Nonlinearity 10 (1997) 1331.
[38] C.G. Goedde, A.J. Lichtenberg, M.A. Lieberman, Physica D 59 (1992) 200.